



Enhancement of second-order nonlinear optical response in boron nitride nanocone: Li-doped effect



Wen-Yong Wang, Na-Na Ma, Cun-Huan Wang, Meng-Ying Zhang, Shi-Ling Sun, Yong-Qing Qiu*

Institute of Functional Material Chemistry, Faculty of Chemistry, Northeast Normal University, Changchun 130024, Jilin, People's Republic of China

ARTICLE INFO

Article history:

Received 5 July 2013

Received in revised form

10 September 2013

Accepted 13 September 2013

Available online 23 September 2013

Keywords:

Electronic structure

DFT

frequency dependent

Li-doped nanomaterial

First hyperpolarizability

ABSTRACT

The unusual properties of Li-doped boron nitride nanomaterials have been paid further attention due to their wide applications in many promising fields. Here, density functional theory (DFT) calculations have been carried out to investigate the second-order nonlinear optical (NLO) properties of boron nitride nanocone (BNNC) and its Li-doped BNNC derivatives. The natural bond orbital charge, electron location function, localized orbital locator and frontier molecular orbital analysis offer further insights into the electron density of the Li-doped BNNC derivatives. The electron density is effectively bounded by the Li atom and its neighboring B atoms. The Li-doped BNNC molecules exhibit large static first hyperpolarizabilities (β_{tot}) up to 1.19×10^3 a.u. for Li@2N-BNNC, 5.05×10^3 a.u. for Li@2B-BNNC, and 1.08×10^3 a.u. for Li@BN-BNNC, which are significantly larger than that of the non-doped BNNC (1.07×10^2 a.u.). The further investigations show that there are clearly dependencies of the first hyperpolarizabilities on the transition energies and oscillator strengths. Moreover, time-dependent DFT results show that the charge transfer from BNNC to Li atom becomes more pronounced as doping the Li atom to BNNC. It is also found that the frequency-dependent effect on the first hyperpolarizabilities is weak, which may be beneficial to experimentalists for designing Li-doped BNNC molecules with large NLO responses.

© 2013 Elsevier Inc. All rights reserved.

1. Introduction

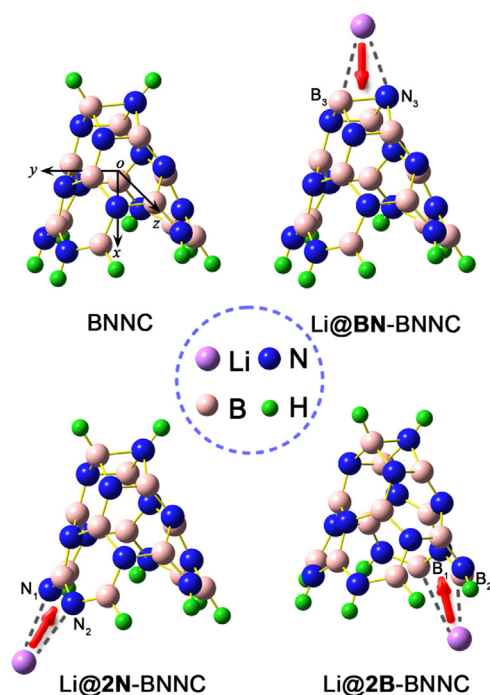
During the past 20 years, great effects have been devoted to design and synthesize high-performance nonlinear optical (NLO) materials for their potential applications in low-cost, high-performance photonic and electro-optical devices [1–10]. Up to now, the effective ways to enhance NLO responses mainly include enhancing the strength of the donor and acceptor [11], enhanced push–pull effects [12,13], twisted π -electron systems [14], introduction of a transition metal atom into the organic compounds [11,15–17], and so forth. Increasingly, recent studies of NLO responses have focused on the materials with Li-doped electride/salt complexes [18–21]. These alkali-metal-doped model systems exhibit very large static first hyperpolarizabilities (β_{tot}). For example, the alkali-doped organic molecules Li@calix[4]pyrrole and the alkali molecule Li⁺(calix-[4]pyrrole)M[−] (M = alkali atoms) have large β_{tot} values (ranging from 10 969 a.u. to 35 934 a.u.) [18,21]. And the β_{tot} value of a very small compound (HCN...Li) with only four atoms is 13979 a.u. [22], which is comparable with that of traditional large donor/acceptor polyenes systems (ranging from 8818 a.u. to 15502 a.u.) [11]. It thus

demonstrates that doping alkali metals into proper organic complexants forms electride and alkali molecules, which is an effective way to enhance static first hyperpolarizability [19].

The first attempts to estimate the magnitude of hyperpolarizabilities of lithiated organic molecules have been carried out by using semiempirical methods [23]. Papadopoulos et al. first investigated the lithiation effect of the conjugated benzenoid ring on the second hyperpolarizability [24]. Champagne et al. investigated the effect of charging on the second hyperpolarizabilities of polyacetylene chains by explicit doping alkali metal atoms [25]. Recently, the lithiation effects on the first hyperpolarizabilities of acene systems with planar π conjugation were investigated by Xu and co-workers [26–28]. Related theoretical studies on boron nitride nanotube (BNNT) have also been recently carried out [29–31]. The results show that BNNT is sensitive to external electron. Paying further attention to the mechanism of the electrical polarization property in boron nitride nanomaterials might open new perspectives to develop their further applications in nanotechnology.

From the above reports and appealing features of boron nitride nanomaterials, we are inspired to probe into the research of the novel boron nitride nanocones (BNNC) with large NLO responses. BNNC is one example for single layer nanostructures of BN and has already been experimentally synthesized and theoretically predicted [32,33]. Up to now, there are various techniques can be used to produce BNNCs, such as reactive ion etching (RIE) [34],

* Corresponding author. Tel.: +86 431 85099291; fax: +86 431 85098768.
E-mail address: qiuyq466@nenu.edu.cn (Y.-Q. Qiu).



Scheme 1. Molecular structures of BNNC and its Li-doped derivatives.

thermal annealing under lithium vapor [35] and chemical vapor deposition with boron and metal oxide as the reactant (BOCVD) [36]. Due to their unique interesting cone-shaped morphologies, greater rigidity, and easier mounting, BNNCs are more potential candidates for field emitters [37] and hydrogen storage materials [33,38] and so forth. However, there is less research on the NLO properties of Li-doped BNNC molecules. Can the first hyperpolarizability be increased when the Li atom doping on BNNC to form a new type of Li salts?

We have proposed a novel way to produce Li@BNNC molecules with good NLO values to answer this question. From the theoretical analyses before [39], it is noted that BNNCs can be generated by curling the white graphene with disclination angle $n \cdot 120^\circ$ in order to form the complete B–N bond. The 240° disclination is the smallest cone geometry ensuring the presence of B–N bonds only. Therefore, in this work, we first focus on the BNNC with 240° disclination angle and a suitable cone height (8.0 \AA) as complexant to design a new type of alkali-metal complexes with large β_{tot} values. The Li@BN-BNNC, Li@2N-BNNC and Li@2B-BNNC were formed by doping the Li atom to the top and two different bottom sides of BNNC, respectively (see Scheme 1). Significantly, it is our expectation that the doping effect on the first hyperpolarizability is great and quite different. Our investigation has focused on the molecular structure, electronic structure, frontier molecular orbital, and nonlinear optical response. The results may be beneficial in both designing high-performance NLO materials and understanding the origin of the interaction between the BNNC and the Li atom.

2. Computational details

It is well known that the choice of suitable method is crucial to generate reliable and accurate results. For calculation methods, the global hybrid generalized gradient approximation M06-2X functional was recommended by Truhlar and Zhao for calculation applications involving main group chemistry, valence and Rydberg electronic excitation energies, and aromatic–aromatic stacking interactions. The M06-2X functional is a highnonlocality functional with double the amount of nonlocal exchange (2X), which

is suitable in this work [40,41]. The optimized geometric structures of BNNC, Li@2N-BNNC, Li@2B-BNNC and Li@BN-BNNC with all real frequencies are obtained at the M06-2X/6-31+G(d) level. Furthermore, the natural bond orbital (NBO), Mayer and Wiberg bond order, electron location function (ELF), localized orbital locator (LOL) and vertical ionization potentials (VIP) are calculated at the same functional and basis set as that used to optimize the geometric structures. With regard to the calculation of the hyperpolarizability, choosing a proper method is important. The conventional DFT methods have been reported to provoke an overestimation of the hyperpolarizabilities [42,43]. The overestimation of the hyperpolarizabilities is expected due to the incorrect electric field dependence modeled by the conventional exchange functional treatments. Highly correlated coupled-cluster methods (such as CCSD, CCSD(T), or even higher CCSDT and CCSDTQ) are known to be generally reliable for calculating the hyperpolarizabilities of molecular systems. However, the use of such high-level methods is still limited to small and medium-sized systems due to the high computing cost. Because of the modest accuracy and computational cost, some hybrid DFT methods have been widely used to predict the optoelectronic properties of molecules. For example, the new hybrid meta exchange correlation functional M06-2X was employed to evaluate the static first hyperpolarizabilities for the long-range interaction system ($\text{Na@C}_{60}\text{C}_{60}\text{@F}$) [44] and the excess electron system (Li@BNNT) [30]. The results show that the static first hyperpolarizabilities of M06-2X method are close to those of MP2 method. To check the consistency of our calculations, the Coulomb-attenuated hybrid exchange–correlation functional (CAM-B3LYP) [45], which combines the hybrid qualities of B3LYP and the long-range correction presented by Tawada et al. [46], has been proposed specifically to calculate the first hyperpolarizabilities (Table S1, supporting information). It is clearly seen that two functionals display the same trend in β values. Thus, the β values are all evaluated at M06-2X/6-31+G(d) level throughout this work by analytical third energy derivatives, which is more efficient and less expensive [47]. The total static first hyperpolarizabilities, β_{tot} , for the studied molecules are defined as:

$$\beta_{tot} = (\beta_x^2 + \beta_y^2 + \beta_z^2)^{1/2} \quad (1)$$

β_x , β_y , and β_z represent the components of the first hyperpolarizability tensors along x -, y -, and z -axis, respectively. The first hyperpolarizability component above is defined by the equation (Eq. (2)):

$$\beta_i = \beta_{iii} + \frac{1}{3} \sum_{i \neq j} [(\beta_{ijj} + \beta_{jij} + \beta_{jji})] \quad i, j = x, y, z \quad (2)$$

where β_{iii} is the diagonal tensor, β_{ijj} or β_{jji} are the off-diagonal tensors. Furthermore, to understand the influence of the dispersion (frequency-dependence) and the effect of the electron correlation on the NLO properties, the frequency-dependent first hyperpolarizabilities ($\beta(\omega)$) were evaluated by couple-perturbed (CP) DFT method with M06-2X functional.

To obtain more insight on the description of the trend of second-order NLO responses, time-dependent density functional theory (TD-DFT) was used to compute the excited states of the studied molecules applying the same theory level used for the calculation of the first hyperpolarizabilities. TD-DFT is one of the most successful and extensively used methods to describe the excited states in quantum chemistry owing to its efficiency and accuracy [48,49]. The hybrid M06-2x functional presents a higher percentage of Hartree–Fock (HF) exchange (54%) and is suitable for applications in many nanoscale molecular systems.

All of the calculations were carried out by using the Gaussian 09W program package [50]. The Mayer and Wiberg bond order, ELF, LOL were carried out using MultiWFN 2.5.2 [51].

Table 1
Important geometrical parameters of three Li-doped BNNC derivatives.

Molecule	Bond	Bond length (Å)	Mayer	Wiberg
Li@2N-BNNC	Li–N ₁	1.846	0.62	0.69
	Li–N ₂	2.079	0.32	0.51
Li@2B-BNNC	Li–B ₁	2.295	0.64	0.67
	Li–B ₂	2.294	0.64	0.67
Li@BN-BNNC	Li–N ₃	1.847	0.55	0.69
	Li–B ₃	2.239	0.44	0.52

3. Results and discussion

3.1. Geometrical structure

The optimized structures of BNNC and its Li-doped derivatives with all real frequencies are obtained at the M06-2X/6-31+G(d) level. The main geometrical parameters of Li@2N-BNNC, Li@2B-BNNC and Li@BN-BNNC are listed in Table 1. As can be seen, the bond lengths of Li–B and Li–N are important, with the range from 1.846 Å to 2.295 Å. The bond lengths of Li–B are shorter than the sum of the van der Waals radii of Li (1.82 Å) and B (2.13 Å). The Li–N has the distances from 1.846 to 2.079 Å, also shorter than the sum of the van der Waals radii of Li (1.82 Å) and N (1.55 Å) [52]. These distances present an effective interaction between Li atom and BNNC structure. On the other hand, it is interesting to note that the bond lengths neighboring the Li atom (i.e., N₁–N₂ for Li@2N-BNNC, B₁–B₂ for Li@2B-BNNC, and B₃–N₃ for Li@BN-BNNC) are generally shorter than those of bond lengths of BNNC (Figure S2, Supporting Information). However, bond lengths far from Li atom (i.e., B₁–B₂ and B₃–N₃ for Li@2N-BNNC, N₁–N₂ and B₃–N₃ for Li@2B-BNNC, N₁–N₂ and B₁–B₂ for Li@BN-BNNC) changes slightly with respect to BNNC. Therefore, doping Li atom does not obviously change the geometrical structure of BNNC far from Li atom

but significantly contracts the structure of BNNC neighboring Li atom.

To reveal the relationship between the electronic structures and the geometric structures of Li-doped BNNC salts, the ELF and LOL analyses over Li@2N-BNNC, Li@2B-BNNC and Li@BN-BNNC were carried out (see Fig. 1). The ELF, proposed initially by Becke [53], was performed to measure electron localization in molecular systems. The LOL was proposed by Schmider and Becke [54] to locate and characterize bond effects in terms of kinetic energy contributions. This function reveals localized electron locations without explicitly obtaining localized orbitals, hence its authors named it the localized orbital locator. For Li@2N-BNNC, both the LOL and ELF maps indicate the weak coordination electron density localization between the Li atom and two N atoms, clearly revealing the Li and N bonding interaction, which is explained by their lower two-center Mayer bond order analysis (see Table 1). The order of the circular three-center bond N₁–Li–N₂ for Li@2N-BNNC is 0.001, which is very lower than that of Li@2B-BNNC (0.123 for the circular three-center bond B₁–Li–B₂). For Li@2B-BNNC, however, a local electron density maximum exists between the Li atom and two B atoms, which show an indication of strong binding effect. The results clearly explain the increasing two-center Mayer bond order of Li–B. Correspondingly, for Li@BN-BNNC, the distribution

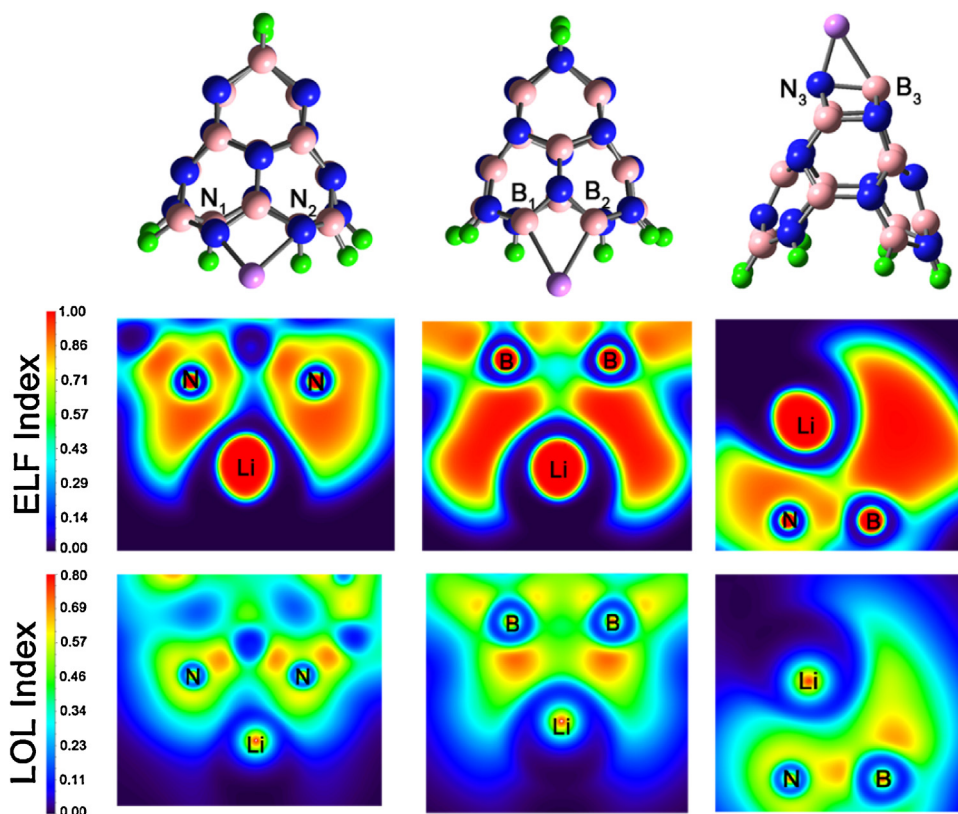


Fig. 1. ELF and LOL analyses over Li@2N-BNNC, Li@2B-BNNC, and Li@BN-BNNC.

Table 2

NBO charges (e) and VIPs (eV) of important atoms in BNNC, Li@2N-BNNC, Li@2B-BNNC and Li@BN-BNNC.

Molecule	BNNC	Li@2N-BNNC	Li@2B-BNNC	Li@BN-BNNC
q(Li)		0.897	0.683	0.819
q(N ₁)	−1.161	−1.318	−1.161	−1.162
q(N ₂)	−1.161	−0.782	−1.161	−1.162
q(B ₁)	0.822	0.825	0.503	0.820
q(B ₂)	0.822	0.820	0.503	0.820
q(N ₃)	−1.158	−1.158	−1.160	−1.313
q(B ₃)	0.729	0.730	0.728	0.674
VIP	9.104	9.386	6.341	6.046

modes of ELF and LOL are located around the B atom. Nevertheless, the electron density localization between Li atom and B, N atoms is low, leading to the middle two-center and three-center (0.009) Mayer bond order. On the basis of the details mentioned above, the distribution of electron density resulting from the ionized Li atom is more centralized around the B atoms in Li@2B-BNNC and Li@BN-BNNC. And more than that, the presence of this loosely delocalized electron density in Li@2B-BNNC and Li@BN-BNNC may lead to the expecting of large NLO responses.

NBO charge analysis has been performed to interpret the interaction between Li atom and the BNNC moiety. From Table 2, the charges of Li atoms are close to +1, 0.897 e for Li@2N-BNNC, 0.683 e for Li@2B-BNNC, and 0.819 e for Li@BN-BNNC, which indicates that the valence electron of the Li atom becomes more diffuse due to the interaction between Li and BNNC. As a result, Li salts (Li@2N-BNNC, Li@2B-BNNC and Li@BN-BNNC) with a Li⁺ cation are formed. Further, the NBO charges of the B and N atoms neighboring Li atom in these Li salts are quite different from that in BNNC, whereas the charges of B, N atoms far from Li atom are almost the same. This further reveals the significant influence of Li atom on structure of BNNC neighboring Li atom. However, the structure of BNNC far from Li atom is slight influenced. It is also important to notice that the charges of the B and N atoms neighboring Li atom become more negative, which indicates the electron density of these B and N atoms are increased by doping one Li atom into the BNNC molecule. Thus, the negative BNNC moiety displays the electron donor character and pronounced charge transfer from BNNC moiety to Li atom is expected. Based on the analysis above, the effect of Li atom on its neighboring B and N atoms is significant and the Li-doped BNNC salts are expected to show some special properties compared with the BNNC.

In order to investigate the stability effect by doping the Li atom to BNNC, the VIP values of BNNC, Li@2N-BNNC, Li@2B-BNNC and Li@BN-BNNC at the M06-2X/6-31+G(d) level are given in Table 2. The VIP values of Li@2N-BNNC, Li@2B-BNNC and Li@BN-BNNC are 9.386 eV, 6.341 eV and 6.046 eV, respectively, which is significantly larger than those of some previously reported Li-doped molecules (3.62 eV for LiCN...Li [29], 4.16 eV for Li@calix[4]pyrroole [18], 3.79 eV for Li-doped fluorocarbon chain [55]). As an important criterion to judge the stability of a molecule, these larger VIP values indicate that the Li-doped BNNC salts are comparatively stable.

3.2. Frontier molecular orbital

The frontier molecular orbitals are often used to obtain qualitative information about the optical and electrical properties of molecules [56]. Further, the highest occupied molecular orbital (HOMO) and the lowest unoccupied molecular orbital (LUMO) energy gap is used to understand the charge transfer interaction that occurs within a molecule. The frontier molecular orbital energies are given in table S3 (Supporting Information). The plots of energy levels, HOMO, and LUMO are also presented in Fig. 2. As shown in Fig. 2, for BNNC, the electronic distribution of HOMO is nearly delocalized over the whole BNNC. Meanwhile, the

electronic distribution of HOMO for Li@2N-BNNC is close to that of BNNC, and we can notice negligible participation of the Li atom. Therefore, one can anticipate that doping Li atom will not cause a significant difference in the HOMO energy of Li@2N-BNNC compared with BNNC. For Li@2B-BNNC and Li@BN-BNNC, however, a significant increase of the electronic distribution in Li atom is notice, resulting the significant lift of the HOMO energy level. Furthermore, the energy gaps between HOMO and HOMO-1 of Li@2B-BNNC and Li@BN-BNNC are large. These large energy gaps may demonstrate the difficulty of the electronic transition from HOMO-1 or lower occupied MOs to unoccupied MOs. Similar to HOMO, for BNNC, the electronic distribution of the LUMO is delocalized over the whole molecule. Unlike the LUMOs of BNNC, the LUMOs of Li@2N-BNNC, Li@2B-BNNC, and Li@BN-BNNC are largely contributed by the Li atom with a little contributed by the B and N atoms connecting to the Li atom. As a result, the LUMO energy levels of Li@2N-BNNC, Li@2B-BNNC, and Li@BN-BNNC get stabilized. Obviously, it can be observed that the Li atom has a significant effect on occupied/unoccupied MOs. Thus, it can be further inferred that the larger contribution of Li atom has not only increased the HOMOs energy but also decreased LUMOs energy, thus leading to the small HOMO-LUMO energy gap in comparison with BNNC. The order of HOMO-LUMO energy gap is progressively decreased as BNNC > Li@2N-BNNC > Li@2B-BNNC > Li@BN-BNNC. The HOMO-LUMO energy gap is the lowest for Li@BN-BNNC, highest for BNNC, and this indicates Li@BN-BNNC should exhibit better NLO property while BNNC should have a poor NLO character. This is well supported by the facts that the lower is the optical gap, the greater will be the nonlinearity.

Previous studies have given a clue that the electronic density of state (DOS) and partial density of state (PDOS) can provide a convenient comprehensive view of the electronic structures and

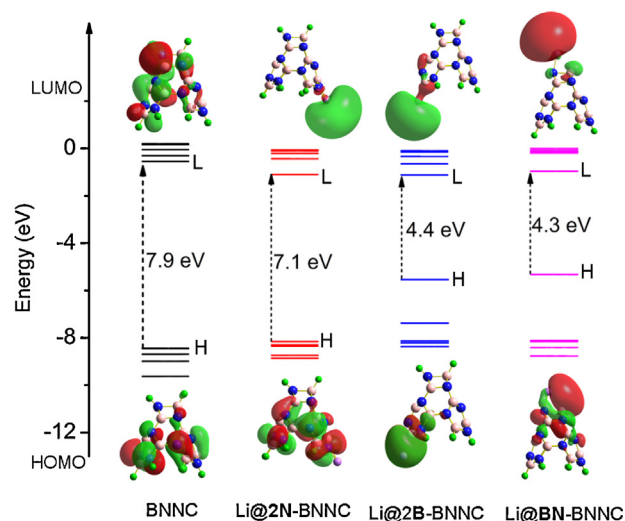


Fig. 2. The frontier molecular orbital energy levels of BNNC, Li@2N-BNNC, Li@2B-BNNC, and Li@BN-BNNC (the electronic distribution of HOMO and LUMO are also presented).

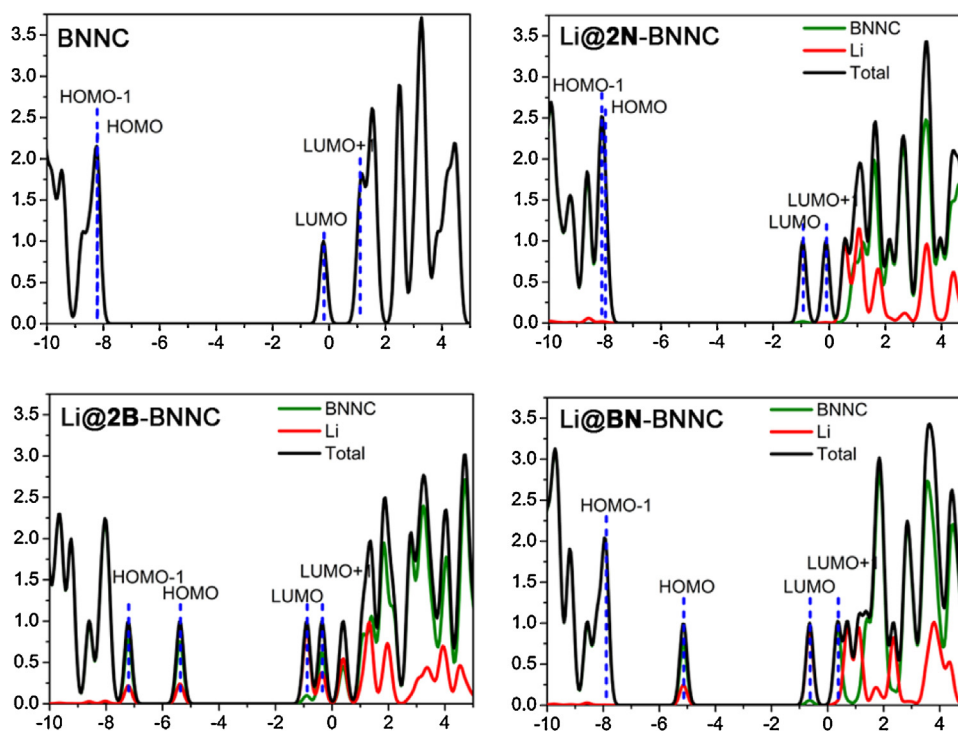


Fig. 3. The density of states (DOSs) and the partial density of states (PDOSs) for BNNC and its Li-doped derivatives.

molecular compositions of compounds. As plotted in Fig. 3, the DOS of BNNC and Li@2N-BNNC show a clear peak formation in the region -7.5 eV to -8.5 eV corresponding to HOMO and HOMO-1 while Li@2B-BNNC and Li@BN-BNNC show a distinct peak formation in the region -4.5 eV to -6.0 eV corresponding to HOMO. It is noted from PDOS that the contribution of Li atom is only 1% to the HOMO level for Li@2N-BNNC. However, the contribution of the Li atom toward HOMOs of Li@2B-BNNC and Li@BN-BNNC is significantly increased (24% and 25%, respectively), which is account for the lift of the HOMO energy level. Finally, for LUMOs, it is worth to be noticed that the near coincidence of the TDOS and PDOS of Li curves reflects the dominant contribution of Li atom (98% Li@2N-BNNC, 90% for Li@2B-BNNC, and 98% for Li@BN-BNNC). The large contribution of Li atom qualitatively explains the moderately decreased LUMO energy level.

3.3. NLO properties

The calculated first hyperpolarizabilities of the studied molecules were obtained by M06-2X functional based on the optimized geometries. All of the main first hyperpolarizabilities are listed in Table 3 and plotted in Fig. 4. As seen, the order of the β_{tot} values is BNNC < Li@2N-BNNC < Li@2B-BNNC < Li@BN-BNNC, which is related to the dispersion of the electron clouds of HOMOs. The β_{tot} value increases as the electronic distribution get more diffused. The β_{tot} value of Li@BN-BNNC is 1.08×10^4 a.u., which

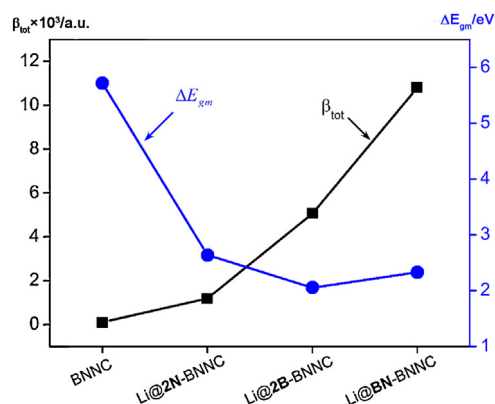


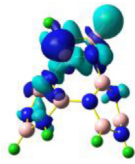
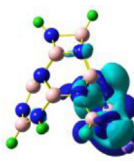
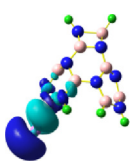
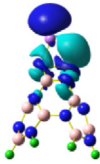
Fig. 4. Relationship between β_{tot} and the difference in transition energy between the ground state and the crucial excited state.

is 101 times larger than that of BNNC (1.07×10^2 a.u.) and also larger than that of the reported cup-like electrode Li@calix[4]-pyrrole (7.33×10^3 a.u.) [18]. Therefore, the loosely electron can effectively enhance the first hyperpolarizability of BNNC. Further, the β_{tot} values of Li@2N-BNNC and Li@2B-BNNC are 1.19×10^3 a.u. and 5.05×10^3 a.u., which increase by about 11 and 47 times as compared to that of BNNC, respectively. Hence, the Li-doped effect greatly increases the static first hyperpolarizabilities.

Table 3
Polarizability α_0 (a.u.), first hyperpolarizabilities β_{tot} (a.u.), electronic spatial extent $\langle R^2 \rangle$ (a.u.) of BNNC, Li@2N-BNNC, Li@2B-BNNC and Li@BN-BNNC at the M06-2X/6-31+G(d) level.

Molecule	BNNC	Li@2N-BNNC	Li@2B-BNNC	Li@BN-BNNC
β_x	-5.00×10^1	5.75×10^2	4.20×10^3	-1.08×10^4
β_y	-9.50×10^1	4.38×10^2	-2.81×10^3	-2.03×10^2
β_z	0.01	-9.47×10^2	-3.5×10^1	1.64×10^2
β_{tot}	1.07×10^2	1.19×10^3	5.05×10^3	1.08×10^4
α_0	1.38×10^2	1.46×10^2	1.56×10^2	1.63×10^2
$\langle R^2 \rangle$	4.87×10^3	4.95×10^3	4.95×10^3	4.97×10^3

Table 4Oscillator strengths (f_{gm}), absorption wavelengths (λ , nm), excited state transition energies (ΔE_{gm} , eV), corresponding dominant MO transitions and EDDM.

Molecule	BNNC	Li@2N-BNNC	Li@2B-BNNC	Li@BN-BNNC
state	3	3	2	1
f_{gm}	0.04	0.01	0.04	0.11
λ	217	471	606	532
ΔE_{gm}	5.72	2.64	2.05	2.33
				
EDDM ^a				
MO transition	H-3 → L (74%)	H-3 → L (41%) H-1 → L (41%)	H → L+1 (41%) H → L+2 (25%)	H → L (86%)

^a Green indicates a decrease of electron density while blue indicates an increase (with isovalue = 0.002 a.u.) (assignment: H = HOMO, L = LUMO, H-1 = HOMO-1, L+1 = LUMO+1, etc.).

How are the β_{tot} values of Li@2N-BNNC, Li@2B-BNNC and Li@BN-BNNC enhanced when the Li atom is doped into the BNNC? In the case of Li-doped BNNCs, firstly, it is possible to understand the controlling factors of β_{tot} values with the relative electronic spatial extent $\langle R^2 \rangle$ [57,58]. The $\langle R^2 \rangle$ value is related to dispersion of electron cloud. The β_{tot} value increases as the electron cloud gets more diffused. As seen from Table 3, the order of $\langle R^2 \rangle$ values is consistent with that of β_{tot} and α_0 values. Furthermore, the $\langle R^2 \rangle$ values are the same order of magnitude, which ranges from 4.87×10^3 a.u. to 4.97×10^3 a.u. Correspondingly, the α_0 values of Li doped molecules ranges from 1.38×10^2 a.u. to 1.63×10^2 a.u. (also the same order of magnitude). Thus, the electronic spatial extent is more important to the polarizability rather than the first hyperpolarizability in this work.

Another approach to evaluate the first hyperpolarizability is from perturbation theory approaches, which expressed the first hyperpolarizability by the “sum-over-states” (SOS) expression. From the complex SOS expression, Oudar and Chemla [59,60] have proposed a simple link between the first hyperpolarizability and a low-lying charge-transfer transition through two-level expression. The two-level expression is as follows:

$$\beta_{tot} \propto \frac{\Delta\mu_{gm}f_{gm}}{\Delta E_{gm}^3} \quad (3)$$

where $\Delta\mu_{gm}$ is the difference between excited and ground state dipole moments, f_{gm} is the oscillator strength, ΔE_{gm} is the transition energy. From the expression, the β_{tot} value is inversely proportional to the cube of transition energy.

The TD-DFT calculations were carried out to obtain the oscillator strengths (f_{gm}), excited state transition energies (ΔE_{gm}) of crucial excited states for all the studied molecules at the TD-M06-2X/6-31+G(d) level. The crucial excited states that significantly contribute to the first hyperpolarizabilities are shown in Table 4. As can be seen from Table 4, the transition energy of BNNC is very large (5.72 eV), which is about 3 times than that of Li@2B-BNNC (2.05 eV). Regardless of all other factors, from Eq. (3), it generates about 27 times increase (very close to the 47 times increase for Li@2B-BNNC as compared to the BNNC) in β_{tot} value. Obviously, the transition energy is one of the most important controlling factors for β_{tot} value. The transition energies of Li@2N-BNNC, Li@2B-BNNC and Li@BN-BNNC are respectively 2.64 eV, 2.05 eV and 2.33 eV, which is much smaller than that of BNNC. Clearly, these pretty small transition energies lead to the considerably large β_{tot} values. The order of the ΔE_{gm} values is as follows: BNNC > Li@2N-BNNC > Li@BN-BNNC > Li@2B-BNNC. It is worth pointing out that the ΔE_{gm} value is inversely proportional to the β_{tot} value of all studied molecules except Li@BN-BNNC (see Fig. 4). Since the ΔE_{gm} value of Li@BN-BNNC is larger than that of Li@2B-BNNC, what causes the larger

β_{tot} value of Li@BN-BNNC? From Table 4, one can see that the f_{gm} value of Li@BN-BNNC is 3 times larger than that of Li@2B-BNNC, thus, leading to the large β_{tot} value. Therefore, the f_{gm} is another important controlling factor for β_{tot} value.

For the purpose of understanding the origin of the second-order NLO response, we focused on analyzing the orbital transition properties associated with the crucial excited states. The calculated vertical transition energies, absorption wavelength, and the composition and percentage of contributions of various configurations to the excitations are listed in Table 4. From Table 4, it can be seen that the excitation of HOMO-3 → LUMO (74%) is responsible for the 217 nm absorption of BNNC. This absorption can be ascribed as $\pi-\pi^*$ transition, which is also supported by the electron density difference maps (EDDM) as shown in Table 4. The EDDM can intuitively demonstrate the electronic transition. The electronic transition from N atoms to B atoms is revealed at the top of BNNC. However, the transition is very mixed, which is not favorable in increasing the β_{tot} value. The 471 nm absorption of Li@2N-BNNC is contributed by the HOMO-3 → LUMO (41%) and HOMO-1 → LUMO (41%) transition. Similarly, such mixed $\pi-\pi^*$ electronic transition is also observed in Li@2N-BNNC, which results in the very small β_{tot} values. In addition, the 606 nm absorption of Li@2B-BNNC is derived from HOMO → LUMO + 1 (41%) and HOMO → LUMO + 2 (25%) transition, while the 532 nm absorption of Li@BN-BNNC is associated with the HOMO → LUMO (86%) transition. The HOMO to LUMO or higher unoccupied MOs transitions in Li@2B-BNNC and Li@BN-BNNC further support the difficulty of the electronic transition from HOMO-1 or lower occupied MOs to unoccupied MOs at the “Frontier Molecular Orbital” section. The EDDMs of Li@2B-BNNC and Li@BN-BNNC illustrate that the character of transition is assigned as BNNC fragment to Li atom charge transfer. The electronic transition from BNNC fragment to Li atom in Li@2B-BNNC and Li@BN-BNNC are more pronounced. The pronounced electronic transition can cause the small transition energy between the ground and the excited states for Li-doped BNNC molecules, thus, leading to the enhanced β_{tot} values.

To make our calculations more useful to experimentalists, we investigated the frequency-dependent first hyperpolarizability by using coupled perturbed Hartree–Fock (CPHF) theory with M06-2X functional and the same basis sets with static first hyperpolarizability calculation. We calculated the frequency-dependent first hyperpolarizability $\beta(-2\omega; \omega, \omega)$ for the second harmonic generation (SHG) and $\beta(-\omega; \omega, \omega)$ for the electro-optical Pockels effect (EOPE). Table 5 listed the estimated values $\beta(-\omega; \omega, \omega)$ and $\beta(-2\omega; \omega, \omega)$ at $\omega = 0.0050, 0.010$, and 0.239 a.u. For BNNC and its Li-doped derivatives, the estimated frequency-dependent $\beta(-2\omega; \omega, \omega)$ values are larger than that of their corresponding $\beta(-\omega; \omega, \omega)$ values. In addition, the values of $\beta(-\omega; \omega, \omega)$ and

Table 5The estimated values of $\beta(-\omega; \omega, 0)$ and $\beta(-2\omega; \omega, \omega)$ (a.u.) at specific frequencies (a.u.).

Molecule	0.0050 (a.u.).		0.0100 (a.u.).		0.0239 (a.u.).	
	$\beta(-\omega; \omega, 0)$	$\beta(-2\omega; \omega, \omega)$	$\beta(-\omega; \omega, 0)$	$\beta(-2\omega; \omega, \omega)$	$\beta(-\omega; \omega, 0)$	$\beta(-2\omega; \omega, \omega)$
BNNC	1.05×10^2	1.05×10^2	1.05×10^3	1.06×10^2	1.07×10^2	1.10×10^2
Li@2N-BNNC	1.20×10^3	1.23×10^3	1.24×10^3	1.41×10^3	1.72×10^3	1.16×10^3
Li@2B-BNNC	4.88×10^3	4.90×10^3	4.94×10^3	5.02×10^3	5.41×10^3	5.91×10^3
Li@BN-BNNC	1.11×10^4	1.12×10^4	1.13×10^4	1.17×10^4	1.24×10^4	1.66×10^4

$\beta(-2\omega; \omega, \omega)$ increase with increasing frequency from $\omega = 0.0050$ to 0.0239 a.u. When comparing the static β_{tot} value, the corresponding $\beta(-\omega; \omega, \omega)$ and $\beta(-2\omega; \omega, \omega)$ values are very close to it, which exhibits the weak frequency-dependent effect on β_{tot} value for BNNC, Li@2B-BNNC, Li@2B-BNNC and Li@BN-BNNC.

4. Conclusions

In the present article, the BNNC and three Li-doped BNNC derivatives have been systematically studied by quantum chemical methods. The results reveal that the doped Li atom has a significant effect on geometry of BNNC neighboring Li atom but has not for BNNC far from Li atom. In the Li-doped BNNC derivatives, the Li atom is ionized to form a cation. NBO charge, ELF, LOL and frontier molecular orbital analysis offer further insights into electron density of Li-doped BNNC molecules, which is effectively bounded by the Li atom and its neighboring B atom, and this highly loose electron density causes a considerably increase in the first hyperpolarizability. The β_{tot} values of Li@2N-BNNC, Li@2B-BNNC, and Li@BN-BNNC are 1.19×10^3 a.u., 5.05×10^3 a.u., and 1.08×10^4 a.u., which increase by about 11, 47, and 101 times as compared to that of BNNC, respectively. Moreover, the TDDFT results indicate that the transition energy becomes smaller as doping the Li atom to BNNC. The EDDM intuitively demonstrates that the small transition energy is due to the pronounced electronic transition between the ground and the excited states. It is also found that the frequency-dependent first hyperpolarizabilities slightly changed with increasing the frequencies, which is beneficial for further theoretical and experimental investigations on the NLO responses of molecules.

The present paper provides quantum mechanical framework for NLO properties of new type Li-doped molecules. It is our hope that this work may evoke one's attention to design new Li-doped BNNC molecules with large NLO responses.

Acknowledgement

We gratefully acknowledge the financial support from the National Natural Science Foundation of China (No. 21173035).

Appendix A. Supplementary data

Supplementary data associated with this article can be found, in the online version, at <http://dx.doi.org/10.1016/j.jmgl.2013.09.008>.

References

- [1] D.F. Eaton, Nonlinear optical materials, *Science* 253 (1991) 281–287.
- [2] S.R. Marder, L.T. Cheng, B.G. Tiemann, A.C. Friedli, M. Blanchard-Desce, J.W. Perry, J. Skindhøj, Large first hyperpolarizabilities in push–pull polyenes by tuning of the bond length alternation and aromaticity, *Science* 263 (1994) 511–514.
- [3] M. Blanchard-Desce, V. Alain, P.V. Bedworth, S.R. Marder, A. Fort, C. Runser, M. Barzoukas, S. Lebus, R. Wortmann, Large quadratic hyperpolarizabilities with donor–acceptor polyenes exhibiting optimum bond length alternation: correlation between structure and hyperpolarizability, *Chem. Eur. J.* 3 (1997) 1091–1104.
- [4] V.M. Geskin, C. Lambert, J.L. Brédas, Origin of high second- and third-order nonlinear optical response in ammonio/borato diphenylpolyene zwitterions: the remarkable role of polarized aromatic groups, *J. Am. Chem. Soc.* 125 (2003) 15651–15658.
- [5] M. Nakano, H. Fujita, M. Takahata, K. Yamaguchi, Theoretical study on second hyperpolarizabilities of phenylacetylene dendrimer: toward an understanding of structure–property relation in NLO responses of fractal antenna dendrimers, *J. Am. Chem. Soc.* 124 (2002) 9648–9655.
- [6] N.J. Long, C.K. Williams, Metal alkynyl σ complexes: synthesis and materials, *Angew. Chem. Int. Ed.* 42 (2003) 2586–2617.
- [7] B. Kirtman, B. Champagne, D.M. Bishop, Electric field simulation of substituents in donor–acceptor polyenes: a comparison with ab initio predictions for dipole moments, polarizabilities, and hyperpolarizabilities, *J. Am. Chem. Soc.* 122 (2000) 8007–8012.
- [8] S.R. Marder, W.E. Torruellas, M. Blanchard-Desce, V. Ricci, G.I. Stegeman, S. Gilmore, J.L. Brédas, J. Li, G.U. Bublitz, S.G. Boxer, large molecular third-order optical nonlinearities in polarized carotenoids, *Science* 276 (1997) 1233–1236.
- [9] F.W. Vance, J.T. Hupp, Probing the symmetry of the nonlinear optic chromophore Ru(trans-4,4'-diethylaminostyryl-2,2'-bipyridine) 32^+ : insight from polarized hyper-rayleigh scattering and electroabsorption (stark) spectroscopy, *J. Am. Chem. Soc.* 121 (1999) 4047–4053.
- [10] A. Plaquet, B. Champagne, F. Castet, L. Ducasse, E. Bogdan, V. Rodriguez, J.L. Pozzo, Theoretical investigation of the dynamic first hyperpolarizability of DHA-VHF molecular switches, *New J. Chem.* 33 (2009) 1349–1356.
- [11] D.R. Kanis, M.A. Ratner, T.J. Marks, Design and construction of molecular assemblies with large second-order optical nonlinearities. Quantum chemical aspects, *Chem. Rev.* 94 (1994) 195–242.
- [12] B.J. Coe, L.A. Jones, J.A. Harris, B.S. Brunschwig, I. Asselberghs, K. Clays, A. Persoons, Highly unusual effects of π -conjugation extension on the molecular linear and quadratic nonlinear optical properties of ruthenium(II) ammine complexes, *J. Am. Chem. Soc.* 125 (2002) 862–863.
- [13] B.J. Coe, S.P. Foxon, E.C. Harper, J. Raftery, R. Shaw, C.A. Swanson, I. Asselberghs, K. Clays, B.S. Brunschwig, A.G. Fitch, Nonlinear optical and related properties of iron(II) pentacyanide complexes with quaternary nitrogen electron acceptor units, *Inorg. Chem.* 48 (2009) 1370–1379.
- [14] J.S. Yang, K.L. Liao, C.Y. Li, M.Y. Chen, Meta conjugation effect on the torsional motion of aminostilbenes in the photoinduced intramolecular charge-transfer state, *J. Am. Chem. Soc.* 129 (2007) 13183–13192.
- [15] S. Di Bella, Second-order nonlinear optical properties of transition metal complexes, *Chem. Soc. Rev.* 30 (2001) 355–366.
- [16] B.J. Coe, Switchable nonlinear optical metallochromophores with pyridinium electron acceptor groups, *Acc. Chem. Res.* 39 (2006) 383–393.
- [17] A. Lachman, Ueber das bewad'sche triäthylaminoxid, *Ber. Dtsch. Chem. Ges.* 33 (1900) 1030–1034.
- [18] W. Chen, Z.R. Li, D. Wu, Y. Li, C.C. Sun, F.L. Gu, The structure and the large nonlinear optical properties of Li@Calix[4]pyrrole, *J. Am. Chem. Soc.* 127 (2005) 10977–10981.
- [19] Z.J. Li, Z.R. Li, F.F. Wang, C. Luo, F. Ma, D. Wu, Q. Wang, X.R. Huang, A dependence on the petal number of the static and dynamic first hyperpolarizability for electroneutral molecules: many-petal-shaped Li-doped cyclic polyamines, *J. Phys. Chem. A* 113 (2009) 2961–2966.
- [20] H.L. Xu, Z.R. Li, D. Wu, B.Q. Wang, Y. Li, F.L. Gu, Y. Aoki, Structures and large NLO responses of new electrides: Li-doped fluorocarbon chain, *J. Am. Chem. Soc.* 129 (2007) 2967–2970.
- [21] W. Chen, Z.R. Li, D. Wu, Y. Li, C.C. Sun, F.L. Gu, Y. Aoki, Nonlinear optical properties of alkali-doped Li+(calix[4]pyrrole) M^- ($M = \text{Li, Na, and K}$): alkali anion atomic number dependence, *J. Am. Chem. Soc.* 128 (2006) 1072–1073.
- [22] W. Chen, Z.R. Li, D. Wu, R.Y. Li, C.C. Sun, Theoretical investigation of the large nonlinear optical properties of (HCN) n clusters with Li atom, *J. Phys. Chem. B* 109 (2004) 601–608.
- [23] M.G. Papadopoulos, S.G. Raptis, I.N. Demetropoulos, S.M. Nasiou, Some organic and organometallic molecules with remarkably large second hyperpolarizabilities, *Theor. Chem. Acc.* 99 (1998) 124–134.
- [24] S.G. Raptis, M.G. Papadopoulos, A.J. Sadlej, Hexalithiobenzene: A molecule with exceptionally high second hyperpolarizability, *Phys. Chem. Chem. Phys.* 2 (2000) 3393–3399.
- [25] B. Champagne, M. Spassova, J.B. Jadin, B. Kirtman, Ab initio investigation of doping-enhanced electronic and vibrational second hyperpolarizability of polyacetylene chains, *J. Chem. Phys.* 116 (2002) 3935–3946.
- [26] Y.Y. Hu, S.L. Sun, S. Muhammad, H.L. Xu, Z.M. Su, How the number and location of lithium atoms affect the first hyperpolarizability of graphene, *J. Phys. Chem. C* 114 (2010) 19792–19798.

- [27] H.L. Xu, Z.R. Li, Z.M. Su, S. Muhammad, F.L. Gu, K. Harigaya, Knot-isomers of Möbius cyclacene: how does the number of knots influence the structure and first hyperpolarizability? *J. Phys. Chem. C* 113 (2009) 15380–15383.
- [28] C.C. Zhang, H.L. Xu, Y.Y. Hu, S.L. Sun, Z.M. Su, Quantum chemical research on structures, linear and nonlinear optical properties of the Li@*n*-acenes salt (*n* = 1, 2, 3, and 4), *J. Phys. Chem. A* 115 (2011) 2035–2040.
- [29] R.L. Zhong, H.L. Xu, S. Muhammad, J. Zhang, Z.M. Su, The stability and nonlinear optical properties: encapsulation of an excess electron compound LiCNLi within boron nitride nanotubes, *J. Mater. Chem.* 22 (2012) 2196–2202.
- [30] R.L. Zhong, H.L. Xu, S.L. Sun, Y.Q. Qiu, Z.M. Su, The excess electron in a boron nitride nanotube: pyramidal NBO charge distribution and remarkable first hyperpolarizability, *Chem. Eur. J.* 18 (2012) 11350–11355.
- [31] F. Ma, Z.J. Zhou, Y.T. Liu, Li₂ trapped inside tubiform [*n*] boron nitride clusters (*n* = 4–8): structures and first hyperpolarizability, *ChemPhysChem* 13 (2012) 1307–1312.
- [32] L. Bourgeois, Y. Bando, S. Shinozaki, A. Kurashima, T. Sato, Boron nitride cones: structure determination by transmission electron microscopy, *Acta Cryst.* 55 (1999) 168–177.
- [33] L. Bourgeois, Y. Bando, W.Q. Han, T. Sato, Structure of boron nitride nanoscale cones: ordered stacking of 240° and 300° disclinations, *Phys. Rev. B* 61 (2000) 7686–7691.
- [34] Y.S. Zou, Y.M. Chong, A.L. Ji, Y. Yang, Q. Ye, B. He, W.J. Zhang, I. Bello, S.T. Lee, The fabrication of cubic boron nitride nanocone and nanopillar arrays via reactive ion etching, *Nanotechnology* 20 (2009) 155305.
- [35] M. Terauchi, M. Tanaka, K. Suzuki, A. Ogino, K. Kimura, Production of zigzag-type BN nanotubes and BN cones by thermal annealing, *Chem. Phys. Lett.* 324 (2000) 359–364.
- [36] C. Zhi, Y. Bando, C. Tang, D. Golberg, Electronic structure of boron nitride cone-shaped nanostructures, *Phys. Rev. B* 72 (245419) (2005) 1–5.
- [37] M. Machado, P. Piquini, R. Mota, Electronic properties of selected BN nanocones, *Mater. Charact.* 50 (2003) 179–182.
- [38] N. Atsushi, O. Takeo, N. Ichihito, Formation and atomic structures of boron nitride nanohorns, *Sci. Technol. Adv. Mater.* 5 (2004) 629–634.
- [39] Y. Tian, R. Wei, V. Eichhorn, S. Fatikow, B. Shirinzadeh, D. Zhang, Mechanical properties of boron nitride nanocones, *J. Appl. Phys.* 111 (104316) (2012) 1–7.
- [40] Y. Zhao, D. Truhlar, The M06 suite of density functionals for main group thermochemistry, thermochemical kinetics, noncovalent interactions, excited states, and transition elements: two new functionals and systematic testing of four M06-class functionals and 12 other functionals, *Theor. Chem. Acc.* 120 (2008) 215–241.
- [41] Y. Zhao, D.G. Truhlar, Density functionals with broad applicability in chemistry, *Acc. Chem. Res.* 41 (2008) 157–167.
- [42] A. Baranowska-Łączkowska, W. Bartkowiak, R.W. Góra, F. Pawłowski, R. Zaleśny, On the performance of long-range-corrected density functional theory and reduced-size polarized LPol-*n* basis sets in computations of electric dipole (hyper)polarizabilities of π -conjugated molecules, *J. Comp. Chem.* 34 (2013) 819–826.
- [43] I.W. Bulik, R. Zaleśny, W. Bartkowiak, J.M. Luis, B. Kirtman, G.E. Scuseria, A. Avramopoulos, H. Reis, M.G. Papadopoulos, Performance of density functional theory in computing nonresonant vibrational (hyper)polarizabilities, *J. Comp. Chem.* 34 (2013) 1775–1784.
- [44] F. Ma, Z.R. Li, Z.J. Zhou, D. Wu, Y. Li, Y.F. Wang, Z.S. Li, Modulated nonlinear optical responses and charge transfer transition in endohedral fullerene dimers Na@C60C60@F with *n*-fold covalent bond (*n* = 1, 2, 5, and 6) and long range ion bond, *J. Phys. Chem. C* 114 (2010) 11242–11247.
- [45] T. Yanai, D.P. Tew, N.C. Handy, A new hybrid exchange-correlation functional using the Coulomb-attenuating method (CAM-B3LYP), *Chem. Phys. Lett.* 393 (2004) 51–57.
- [46] Y. Tawada, T. Tsuneda, S. Yanagisawa, T. Yanai, K. Hirao, A long-range-corrected time-dependent density functional theory, *J. Chem. Phys.* 120 (2004) 8425–8433.
- [47] P. Chopra, L. Carlucci, H.F. King, P.N. Prasad, Ab initio calculations of polarizabilities and second hyperpolarizabilities in organic molecules with extended π -electron conjugation, *J. Chem. Phys.* 93 (1989) 7120–7130.
- [48] K. Zheng, J. Wang, Y. Shen, D. Kuang, F. Yun, Electronic structures and related properties of complexes M(bpy)₃*n* (M = Re, Os, and Ir; *n* = 1, 2, and 3, respectively), *J. Phys. Chem. A* 105 (2001) 7248–7253.
- [49] A. Vlček, S. Zálaiš, A comments on “theoretical studies of ground and excited electronic states in a series of halide rhenium(I) bipyridine complexes”, *J. Phys. Chem.* 109 (2005) 2991–2992.
- [50] M.J. Frisch, et al., Gaussian 09W, revision A.01, Gaussian Inc., Wallingford, CT, 2009.
- [51] T. Lu, F. Chen, Multiwfn: a multifunctional wavefunction analyzer, *J. Comput. Chem.* 33 (2012) 580–592.
- [52] A. Bondi, van der Waals volumes radii, *J. Chem. Phys.* 68 (1964) 441–451.
- [53] A.D. Becke, K.E. Edgecombe, A simple measure of electron localization in atomic and molecular systems, *J. Chem. Phys.* 92 (1990) 5397–5403.
- [54] H.L. Schmider, A.D. Becke, Chemical content of the kinetic energy density, *J. Mol. Struct.: THEOCHEM* 527 (2000) 51–61.
- [55] X. Blase, A. Rubio, S.G. Louie, M.L. Cohen, Stability and band gap constancy of boron nitride nanotubes, *Europhys. Lett.* 28 (1994) 335–340.
- [56] R.V. Solomon, P. Veerapandian, S.A. Vedha, P. Venuvanalingam, Tuning nonlinear optical and optoelectronic properties of vinyl coupled triazene chromophores: a density functional theory and time-dependent density functional theory investigation, *J. Phys. Chem. A* 116 (2012) 4667–4677.
- [57] A. Fkyerat, A. Guelzim, F. Baert, J. Zyss, A. Périgaud, Assessment of the polarizabilities (α β) of a nonlinear optical compound [N-(4-nitrophenyl)-(1)-prolinol] from an experimental electronic density study, *Phys. Rev. B* 53 (1996) 16236–16246.
- [58] D. Scuderi, A. Paladini, M. Satta, D. Catone, S. Piccirillo, M. Speranza, A.G. Guidoni, Chiral aggregates of indan-1-ol with secondary alcohols and water: laser spectroscopy in supersonic beams Guidoni, *Phys. Chem. Chem. Phys.* 4 (2002) 4999–5003.
- [59] J.L. Oudar, Optical nonlinearities of conjugated molecules Stilbene derivatives and highly polar aromatic compounds, *J. Chem. Phys.* 67 (1977) 446–457.
- [60] J.L. Oudar, D.S. Chemla, Hyperpolarizabilities of the nitroanilines and their relations to the excited state dipole moment, *J. Chem. Phys.* 66 (1977) 2664–2668.